ENCIT 2018

ABCM Associação Brasileira de Engenharia e Ciências Mecânicas

17th Brazilian Congress of Thermal Sciences and Engineering
November 25th-28th, 2018, Águas de Lindóia, SP, Brazil

ENCIT-2018-0187
Assessment of Thermoacoustic Combustion Instabilities in Liquid Rocket Engines Using the Partially Stirred Reactor Combustion Model

Mateus Grassano Lattari
Washington Orlando Irrazabal Bohorquez
Federal University of Juiz de Fora
mateus.grassano@engenharia.ufjf.br, wirraz@engenharia.ufjf.br

Marco Aurélio da Cunha Alves
Federal University of Juiz de Fora
marco.alves@engenharia.ufjf.br

Abstract. *The purpose of this work is the modeling and simulation of hydrogen-oxygen components mixing and chemically reacting in liquid rocket combustion chambers using OpenFOAM. It is a free, open source CFD software capable of simulating complex fluid flows involving heat transfer, chemical reactions, turbulence. The numerical assessment was performed using reactingFoam, a solver based in the Favre-Navier-Stokes equations. As part of the numerical results can be mentioned the pressure oscillations acoustic waves and the speed oscillation patterns in the rocket combustion chamber.*

Keywords: *combustion, instabilities, rocket, reactingFoam, reactor.*

1. INTRODUCTION

Liquid rocket engines are the mean of propulsion used in rockets that almost daily launch many satellites into orbit. These engines are based in the chemical reactions of combustion between two liquid species: one fuel and an oxidizer. The reactants are initially stored in the liquid cryogenic state. The development of combustion process involves many complex processes, such as: turbulence, atomization and reactive flow. The occurrence of these processes can generate acoustic pressure waves and thermal oscillations in the combustion chamber (Wang (2016)). Combustion instabilities result from coupling between the combustion process and the fluid dynamics of the propulsion system. That is so because they make the combustion process become unstable and this instability can generate chamber pressure oscillations. The frequency and amplitude of these oscillations produce severe vibration and grossly increased heat transfer. This is often sufficient to melt and destroy sections of the rocket combustion chamber (Harrje (1972)). The mathematical modeling of this phenomena was first studied in the 1950s by Crocco (1953) and Summerfield (1951). It was developed many analytical equations that were firstly organized in 1964 by the NASA report Harrje (1972). In 90s Young (1995) made another report reorganizing the out coming advances in the field until the date of his work.

The development of the Computational Fluid Dynamics allowed the liquid rocket instability process to be modeled with computational simulations (Chen *et al.* (2011), Cheng and Farmer (2006)), for example, the conservation differential equations started to be solved using discrete iterative methods, such as finite volume. The codes for solving these equations are known as solvers. These solvers were initially programmed to solve specific problems and their development was first made by space agencies and research institutions. In another hands, the capability of those solvers became interesting to commercial and industrial applications and then they started to be sold in packages such as Ansys, Comsol, and others. Commercial solvers are made in such way that one was not allowed to see their source code, implying that no changes could be made in the way these equations were solved and that the deep learning of the processes would remain unknown. However, the community of CFD direct created an opensource CFD platform called Open Formula Operations, Arithmetic and Matrices, the OpenFOAM. As these solvers use free source codes written in C++ many users could create new solvers and add new capabilities to the platform. This development allowed the creation of many combustion solvers. In this present work, the reactingFoam solver is used for the simulation of an LH2-LOX rocket engine. These choices have been made due to the extensive literature available for this case (Tao and Dongmei (2012), Invigorito *et al.* (2014), Smirnov *et al.* (2014)). Currently, many researchers and students around the world use the OpenFoam for the study of combustion instabilities in rocket combustion chambers.

As previously stated, this work aims to show the thermal and acoustical oscillations developed in the rocket combustion chamber. In the next section, the mathematical background of the numerical simulation considering the analytical

equations of chemical reactions in liquid rocket engines are showed. As part of the outcomes, a prediction of both the stable and unstable pressure fluctuations and flow speed is presented.

2. METHODOLOGY

2.1 Theoretical methodology

The simulation was performed using a modification of the DLR_A_LTS template includes in the OpenFOAM reactingFoam tutorials. The solver was chosen based On the fact that it uses the Favre-Navier-Stokes equations, shown in equations: 1 and 2. These equations consider the fluctuating values of the variables. Those fluctuations consider the Favre average for the values, these averages takes places in the application of the Partially Stirred Combustor Method(PaSCM) or Partially Stirred Reactor. The method considers that the combustor is not completely stirred because this fact would imply that only the chemical kinetic would play a role in the reactions. Nevertheless, the turbulence cannot be considered in every molecule because of the almost infinity computational time, for this purpose the Favre average is used in the equations 1 and 2. This is also important in the compressible reactive turbulent flow considered in this present work because these fluctuations coupled with the turbulence generate the speed and pressure oscillations (Wang (2016)). These assumptions were made in accordance with Gonzalez (2017). He developed a combustion instability model for an internal combustion engine. The pressure oscillations produce acoustic fluctuations and this causes enough turbulent disturbances to develop combustion instabilities.

$$\frac{\partial Q}{\partial t} + \frac{\partial (E - E_v)}{\partial x} + \frac{\partial (F - F_v)}{\partial y} + \frac{\partial (G - G_v)}{\partial z} = H \tag{1}$$

where:

$$Q = \begin{bmatrix} \widetilde{\rho} \\ \overline{\rho}\widetilde{u} \\ \overline{\rho}\widetilde{v} \\ \overline{\rho}\widetilde{w} \\ \overline{\rho}\widetilde{e} \\ \overline{\rho}\widetilde{Y}_i \end{bmatrix} \; E = \begin{bmatrix} \overline{\rho}\widetilde{u} \\ \overline{\rho}\widetilde{u} + \overline{p} \\ \overline{\rho}\widetilde{u}\widetilde{v} \\ \overline{\rho}\widetilde{u}\widetilde{w} \\ \widetilde{u}(\overline{\rho}\widetilde{e} + \overline{p}) \\ \overline{\rho}\widetilde{u}\widetilde{Y}_i \end{bmatrix} \; F = \begin{bmatrix} \overline{\rho}\widetilde{v} \\ \overline{\rho}\widetilde{v}\widetilde{u} \\ \overline{\rho}\widetilde{v}\widetilde{v} + \overline{p} \\ \overline{\rho}\widetilde{v}\widetilde{w} \\ \widetilde{v}(\overline{\rho}\widetilde{e} + \overline{p}) \\ \overline{\rho}\widetilde{v}\widetilde{Y}_i \end{bmatrix} \; G = \begin{bmatrix} \overline{\rho}\widetilde{w} \\ \overline{\rho}\widetilde{w}\widetilde{u} \\ \overline{\rho}\widetilde{w}\widetilde{v} \\ \overline{\rho}\widetilde{w}\widetilde{w} + \overline{p} \\ \widetilde{w}(\overline{\rho}\widetilde{e} + \overline{p}) \\ \overline{\rho}\widetilde{w}\widetilde{Y}_i \end{bmatrix} \; E_v = \begin{bmatrix} 0 \\ \overline{\tau}_{xx} \\ \overline{\tau}_{xy} \\ \overline{\tau}_{xz} \\ \widetilde{u}\overline{\tau}_{xx} + \widetilde{v}\overline{\tau}_{xy} + \widetilde{w}\overline{\tau}_{xz} - \widetilde{q}_x \\ \overline{\rho}_i \overline{D}_{imi} \frac{\widetilde{Y}_i}{\partial x} \end{bmatrix} \tag{2}$$

$$F_v = \begin{bmatrix} 0 \\ \overline{\tau}_{yx} \\ \overline{\tau}_{yy} \\ \overline{\tau}_{yz} \\ \widetilde{u}\overline{\tau}_{xy} + \widetilde{v}\overline{\tau}_{yy} + \widetilde{w}\overline{\tau}_{yz} - \widetilde{q}_y \\ \overline{\rho}_i \overline{D}_{imi} \frac{\widetilde{Y}_i}{\partial y} \end{bmatrix} \; G_v = \begin{bmatrix} 0 \\ \overline{\tau}_{zx} \\ \overline{\tau}_{zy} \\ \overline{\tau}_{zz} \\ \widetilde{u}\overline{\tau}_{zx} + \widetilde{v}\overline{\tau}_{zy} + \widetilde{w}\overline{\tau}_{zz} - \widetilde{q}_z \\ \overline{\rho}_i \overline{D}_{imi} \frac{\widetilde{Y}_i}{\partial z} \end{bmatrix} \; H = \begin{bmatrix} S_{d,m} \\ S_{d,u} \\ S_{d,v} \\ S_{d,w} \\ S_{d,h} \\ \widetilde{\omega}_i \end{bmatrix}$$

The turbulence is solved using the $k - \epsilon$ model includes in the pimpleFOAM solver. This solver is used in the source code of reactingFOAM in order to solve the flow field. This turbulence model is derived from the Favre average, as shown in the equations: 1 and 2. This development is shown in equation 3 to 8.

$$\frac{\partial \overline{\rho}}{\partial t} + \frac{\partial}{\partial t}(\overline{\rho}\widetilde{u}_j) = 0 \tag{3}$$

$$\frac{\partial}{\partial t}(\overline{\rho}\widetilde{u}_i) + \frac{\partial}{\partial X_j}(\overline{\rho}\widetilde{u}_j\widetilde{u}_i) = \frac{\partial}{\partial X_j}(\mu e \frac{\partial \widetilde{u}_i}{\partial X_j}) + S_{u_i} \tag{4}$$

$$\frac{\partial}{\partial t}(\overline{\rho}k) + \frac{\partial}{\partial X_j}(\overline{\rho}\widetilde{u}_j k) = \frac{\partial}{\partial X_j}(\frac{\mu_e}{\sigma_R}\frac{\partial k}{\partial X_j}) + G_k - \overline{\rho}\epsilon \tag{5}$$

$$\frac{\partial}{\partial t}(\overline{\rho}\epsilon) + \frac{\partial}{\partial X_j}(\overline{\rho}\widetilde{u}_j \epsilon) = \frac{\partial}{\partial X_j}(\frac{\mu_e}{\sigma_\epsilon}\frac{\partial \epsilon}{\partial X_j}) + \frac{\epsilon}{k}(C_1 G_k - C_2\overline{\rho}\epsilon) \tag{6}$$

$$\frac{\partial}{\partial t}(\overline{\rho}\widetilde{Z}) + \frac{\partial}{\partial X_j}(\overline{\rho}\widetilde{u}_j \widetilde{Z}) = \frac{\partial}{\partial X_j}(\frac{\mu_e}{\sigma_Z}\frac{\partial \widehat{Z}}{\partial X_j}) \tag{7}$$

$$\frac{\partial}{\partial t}(\overline{\rho}g) + \frac{\partial}{\partial X_j}(\overline{\rho}\widetilde{u}_j g) = \frac{\partial}{\partial X_j}(\frac{\mu_e}{\sigma_g}\frac{\partial g}{\partial X_j}) + C_{g1}\mu_t(\frac{\partial \widehat{Z}}{\partial X_j})^2 - C_{g2}(\frac{\overline{\rho}g\epsilon}{k}) \tag{8}$$

The set of equations are solved using the Finite Elements Method present as a utility in OpenFoam. The development of the method is not shown in this work, nevertheless, it can be consulted in the extensive work of basic books about this method. Example: Moukalled *et al.* (2015).

As exposed the reaction mechanism is the $H_2 + O_2$ combustion, in which the final product is H_2O. Therefore there are plenty of reactions in this mechanism that generates intermediately radicals. Those equations play a central role in the equilibrium dynamics in this simulation. The mechanism was developed for Conaire *et al.* (2004) and it was integrated into Chemkim table in the reactingFoam solver. It is shown in figure 1.

	Reaction	A	n	E_a	Ref.
		H_2/O_2 chain reactions			
1	$\dot{H} + O_2 = \dot{O} + \dot{O}H$	1.91×10^{14}	0.00	16.44	[39]
2	$\dot{O} + H_2 = \dot{H} + \dot{O}H$	5.08×10^{4}	2.67	6.292	[40]
3	$\dot{O}H + H_2 = \dot{H} + H_2O$	2.16×10^{8}	1.51	3.43	[41]
4	$\dot{O} + H_2O = \dot{O}H + \dot{O}H$	2.97×10^{6}	2.02	13.4	[42]
		H_2/O_2 dissociation/recombination reactions			
5[a]	$H_2 + M = \dot{H} + \dot{H} + M$	4.57×10^{19}	−1.40	105.1	[43]
6[b]	$\dot{O} + \dot{O} + M = O_2 + M$	6.17×10^{15}	−0.50	0.00	[43]
7[c]	$\dot{O} + \dot{H} + M = O\dot{H} + M$	4.72×10^{18}	−1.00	0.00	[43]
8[d,e]	$\dot{H} + \dot{O}H + M = H_2O + M$	4.50×10^{22}	−2.00	0.00	[43] ×2.0
		Formation and consumption of $H\dot{O}_2$			
9[f,g]	$\dot{H} + O_2 + M = H\dot{O}_2 + M$	3.48×10^{16}	−0.41	−1.12	[44]
	$\dot{H} + O_2 = H\dot{O}_2$	1.48×10^{12}	0.60	0.00	[45]
10	$H\dot{O}_2 + \dot{H} = H_2 + O_2$	1.66×10^{13}	0.00	0.82	[6]
11	$H\dot{O}_2 + \dot{H} = \dot{O}H + \dot{O}H$	7.08×10^{13}	0.00	0.30	[6]
12	$H\dot{O}_2 + \dot{O} = \dot{O}H + O_2$	3.25×10^{13}	0.00	0.00	[46]
13	$H\dot{O}_2 + \dot{O}H = H_2O + O_2$	2.89×10^{13}	0.00	−0.50	[46]
		Formation and consumption of H_2O_2			
14[h]	$H\dot{O}_2 + H\dot{O}_2 = H_2O_2 + O_2$	4.2×10^{14}	0.00	11.98	[47]
	$H\dot{O}_2 + H\dot{O}_2 = H_2O_2 + O_2$	1.3×10^{11}	0.00	−1.629	[47]
15[i,f]	$H_2O_2 + M = \dot{O}H + O\dot{H} + M$	1.27×10^{17}	0.00	45.5	[48]
	$H_2O_2 = \dot{O}H + O\dot{H}$	2.95×10^{14}	0.00	48.4	[49]
16	$H_2O_2 + \dot{H} = H_2O + \dot{O}H$	2.41×10^{13}	0.00	3.97	[43]
17	$H_2O_2 + \dot{H} = H_2 + H\dot{O}_2$	6.03×10^{13}	0.00	7.95	[43] × 1.25
18	$H_2O_2 + \dot{O} = \dot{O}H + H\dot{O}_2$	9.55×10^{06}	2.00	3.97	[43]
19[h]	$H_2O_2 + \dot{O}H = H_2O + H\dot{O}_2$	1.0×10^{12}	0.00	0.00	[50]
	$H_2O_2 + \dot{O}H = H_2O + H\dot{O}_2$	5.8×10^{14}	0.00	9.56	[50]

Figure (1) Reaction mechanism of the combustion process. Source: Conaire *et al.* (2004)

2.2 Computational methodology

In order to simulate a liquid rocket combustion chamber a 2D model is considered, the thickness is still shown in the model, this was necessary for other to adaptive the model to the OpenFOAM solver, because it is a 3D solver, however the thickness is much smaller than the other dimensions creating an approximation of a 2D model. The geometry represents a cylindrical section of a one injector model of a liquid rocket combustion chamber, it also worth to be mentioned that the geometry was modeled using the blender free software in a .stl format. In the source code of the .stl files, the boundary conditions were designated. There seven boundaries, this number is important because of the turbulent kinematic viscosity condition that was used as a boundary condition in the near injection region.

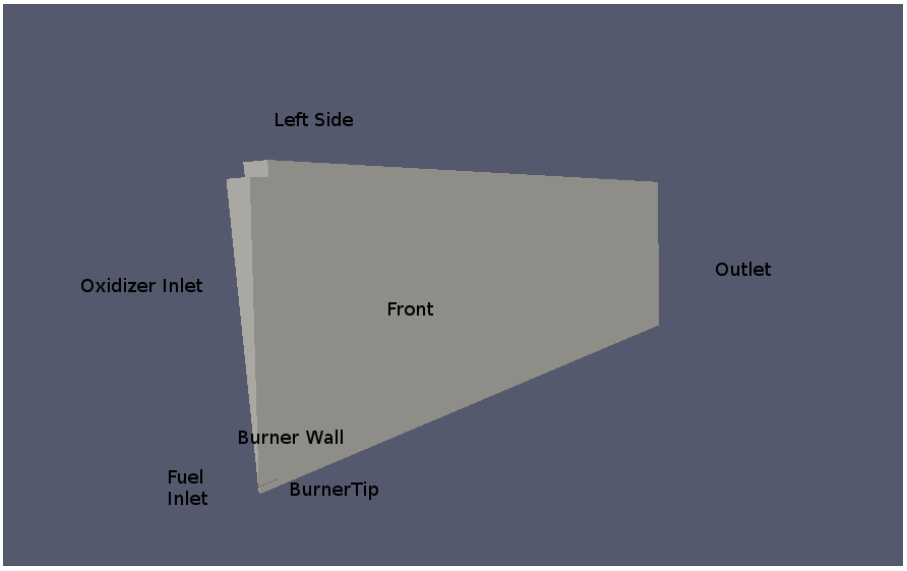

Figure (2) Boundaries visualization in the .stl rendered by Blender

The .stl files are exported to the OpenFOAM case directory. A meshing discretization is performed by the SnappyHexMesh, a utility also from OpenFoam. It is possible to obtain a structured mesh, as shown in Figure 3.

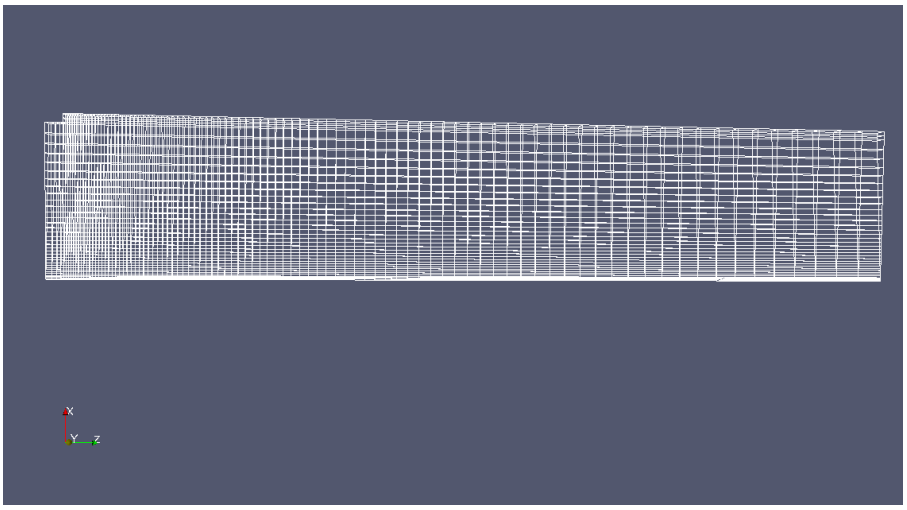

Figure (3) Mesh generated by snappyHexMesh

The simulation was performed using 65100 iterations because, after this step, the simulation became steady. The results were first post-processed using the *paraFOAM* platform, in the second time the results were exported for a *python* script created by the authors for graphic analysis.

3. RESULTS

The simulation performed allowed many interesting results about the combustion process in accordance with the objectives proposed in this paper. The main goals are the visualization and quantification of the pressure and velocity oscillations in the process that were obtained for this computational simulation. The results are divided in the following subsection: Speed and velocity oscillations and Pressure oscillations.

3.1 The speed and velocity oscillations

The first of the results is a contour map of the temporal progression of the simulation that was carried out, this result can be seen in figure 4. This data follows the magnitude of the speed in the $\vec{z}$ direction.

(a) Initial condition,t=0

(b) After ignition flow, t=1000s

(c) t=3000s

(d) t=5000s

(e) t=9000s

(f) t=10000s

Figure (4) Development of the flow with respect to the U (Z direction) magnitude

The result can be best observed by plotting the velocity streamlines overlaid to the speed in $\vec{z}$ direction. As it can be seen in figure 5 there are vorticities patterns in the above region of the combustion flame. It is plausible because of the turbulence and also because of the radicals that are being formed in the below region. As the combustion process accelerates the flow it creates vorticities in the fluid that is initially unaccelerated. Also as the combustion process rapidly advances the fluid to a turbulent state, it is reasonable to consider the turbulence model contribution to the process.

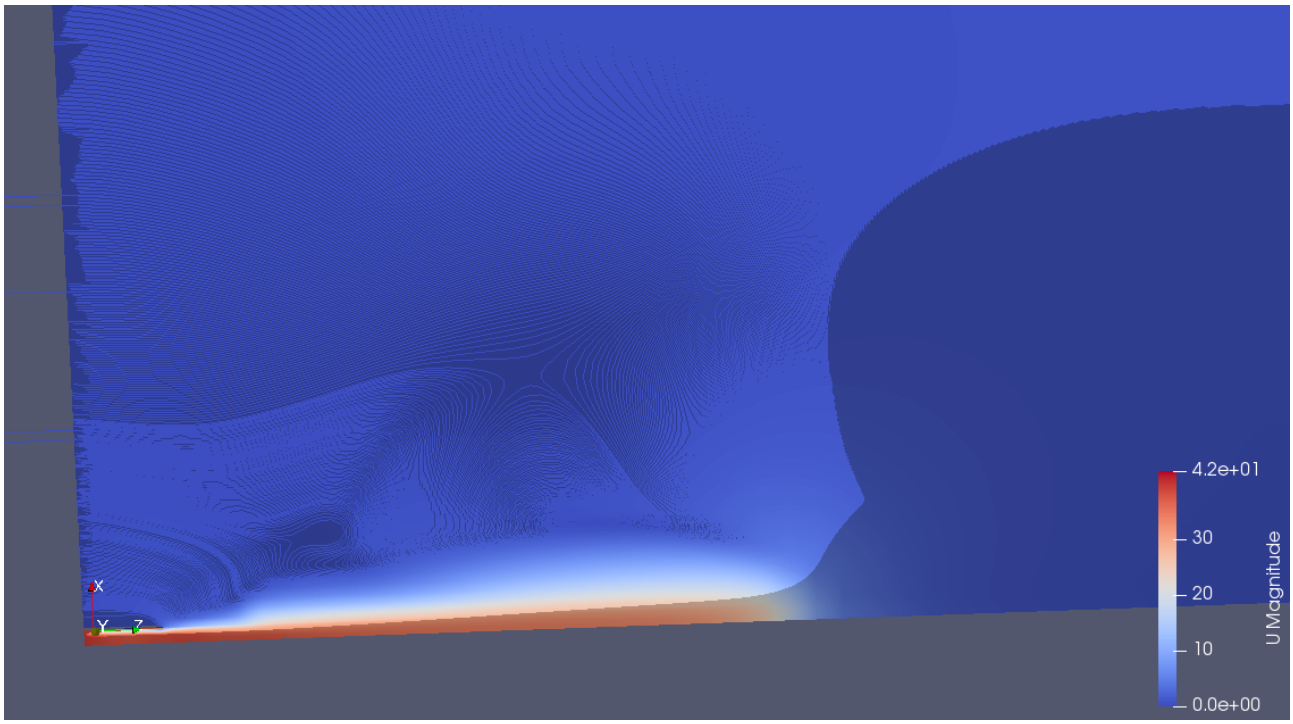

Figure (5) Speed streamlines in the Combustion Chamber after the combustion ignition in the near injector region

A closer observation of the near injector region can lead to the plotting of the speed oscillations with respect to the number of iterations, as shown in figure 6. This result shows agreement with the observed in the extensive bibliography revision present in the first section of this paper and especially there were agreements with the patterns presented by Noiray *et al.* (2008).

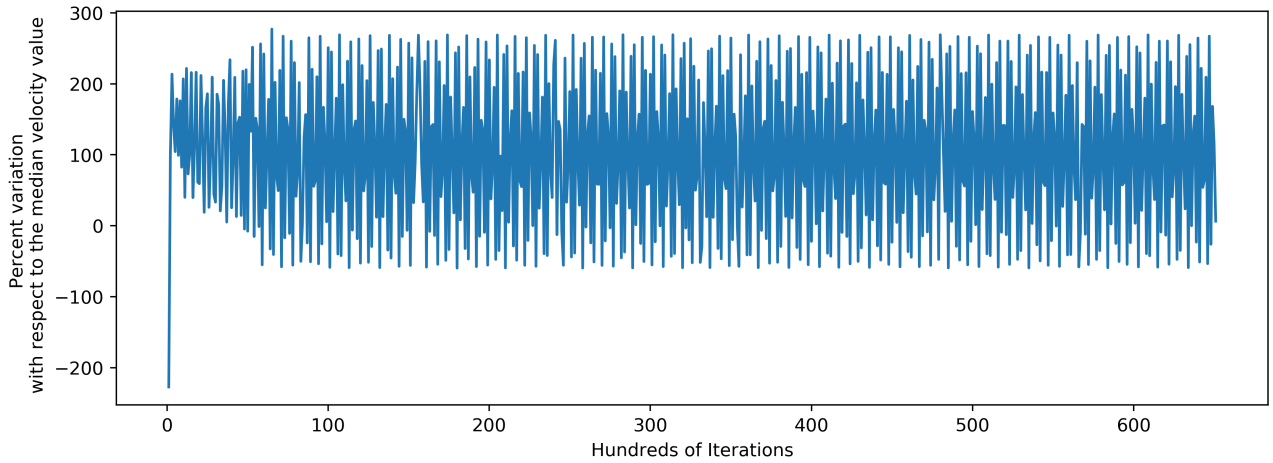

Figure (6) Percent velocity variations relative to the medium value, versus the temporal interactions

An interesting analysis of the graph exposed in 6 is performed in Figure 7. In this analysis, it is applied the Fast Fourier Transformation (FFT) in the pressure oscillation data and the result is plotted with respect to the normalized frequency.

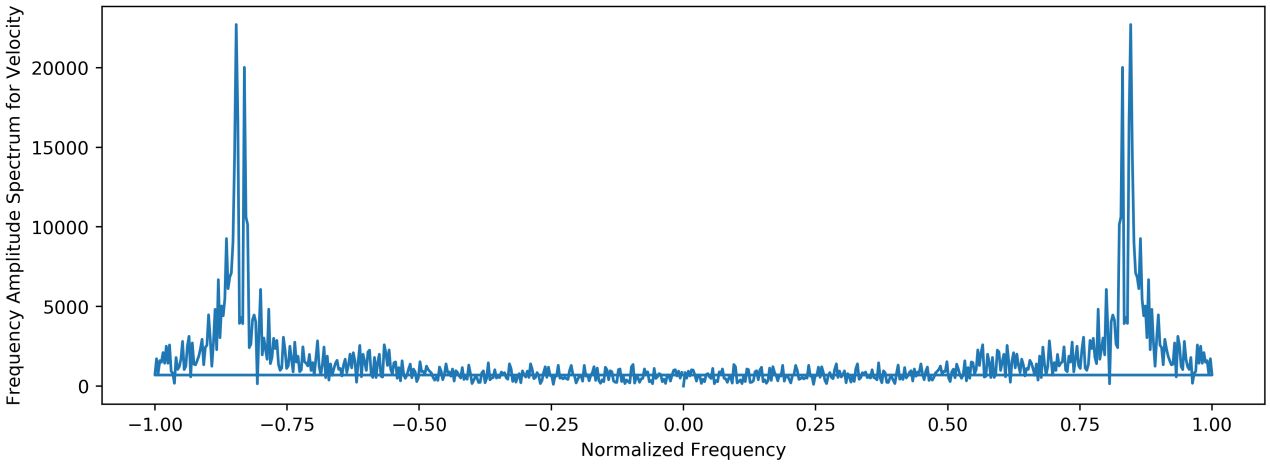

Figure (7) Figure 6 data in frequency normalized domain

The graph (figure 7) allows one to observe the frequency amplitude peaks. Those peaks are the result of the ignition of the reactive pressure. This ignition occurs due to a defined region with high initial temperature.

3.2 The pressure oscillations

As shown for the velocity and speed oscillation the temporal progression image with the pressure, shown in figure 8. Differently, of the previous temporal progression, this one will include the streamline of pressure overlaid in every picture, this was necessary due to the fact that pressure is a scalar.

(a) Initial condition,t=0

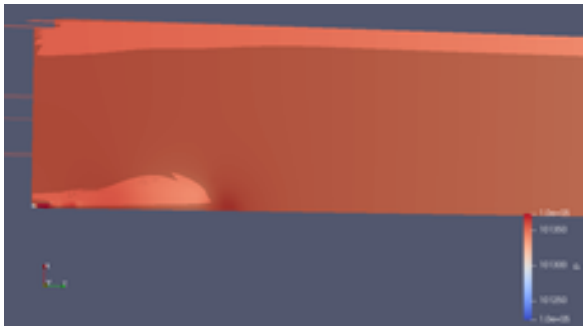

(b) After ignition flow, t=1000s

(c) t=3000s

(d) t=4000s

(e) t=5000s

(f) t=10000s

Figure (8) Development of the flow with respect to the pressure magnitude

It is possible to observe that there is a global peak of pressure in figure 8.b, this occurred because of the combustion stream after the ignition process. The other pictures show the movement of the streamlines as the combustion process takes place. In the last time, Figure 8.f, there is an equalization of the pressure.

The next picture, as has been conducted for the previous analysis, shows a closer view to the pressure oscillation using the pressure streamlines overlaid to the contours, figure 9.

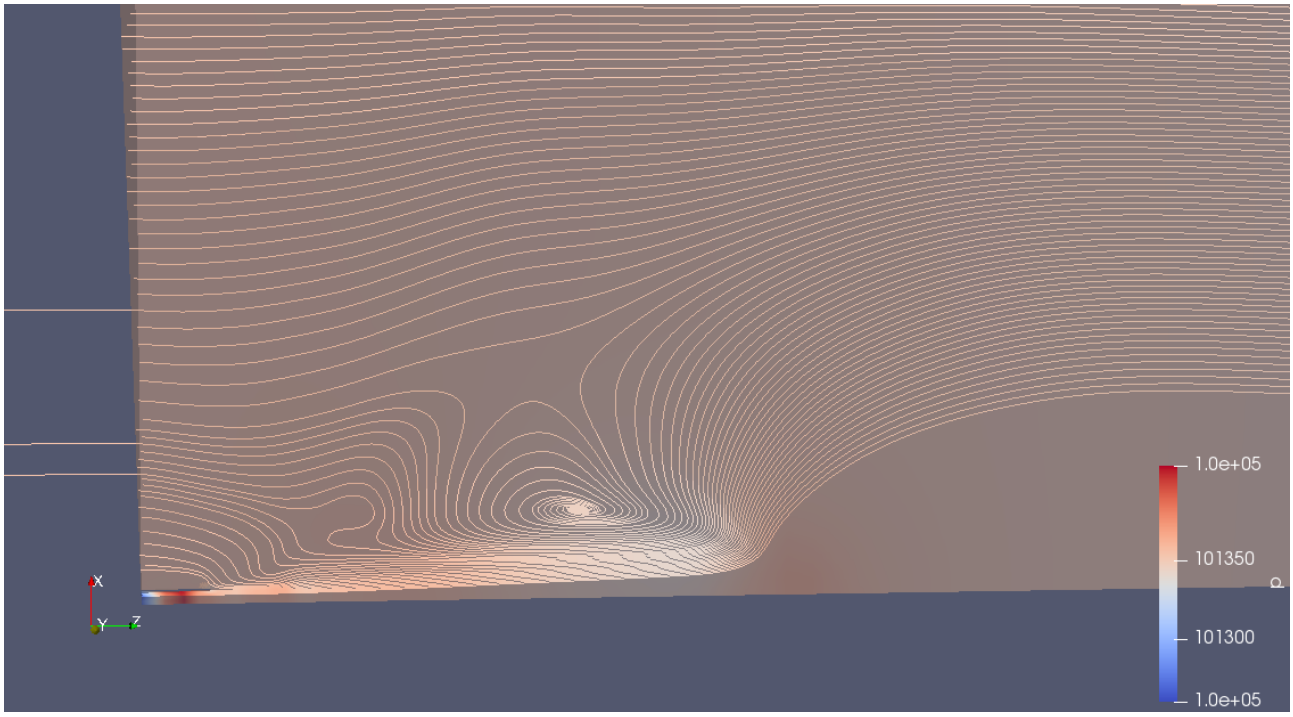

Figure (9) Pressure streamlines in the Combustion Chamber after the combustion ignition in the near injector region

It is very clear that there are vorticities of the streamlines in the same regions that were obtained for the velocity. The next graph shows the pressure oscillation with respect to the interactions, figure 10. This result is obtained, again, in the same near injection region as they have been obtained for the speed, Figure 7.

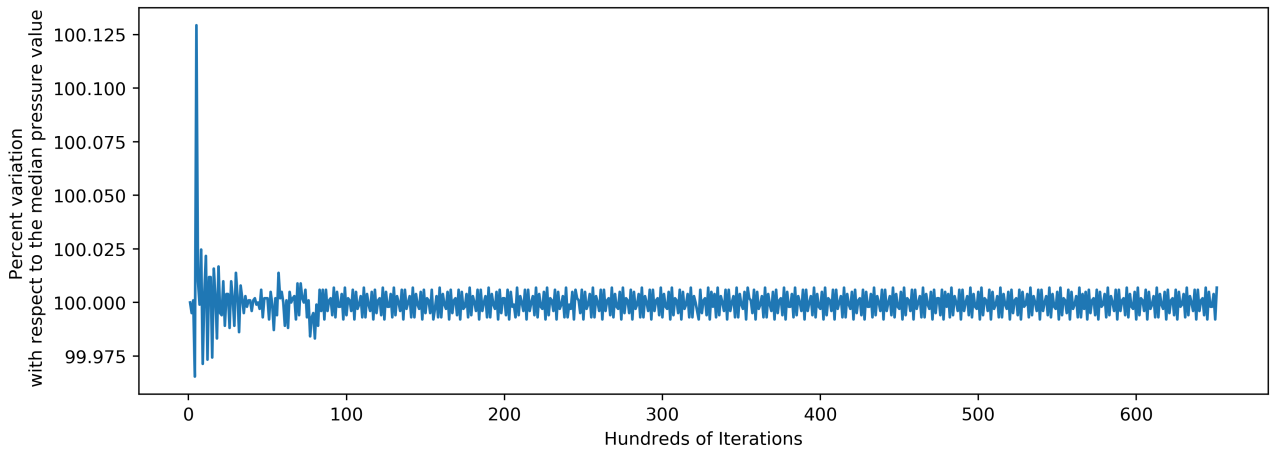

Figure (10) Percent velocity variations relative to the medium value, versus the temporal interactions

This time the pressure plots allows one to observe a well-posed peak in the pressure valuer for the combustion ignition process. After this, the pressure amplitude maintains a pattern until the last iterations. Nevertheless, those values are also analyzed using FFT. It is shown in figure 11. The graph shows agreements with the velocity one. It is observed that the peaks occur in the same normalized frequencies.

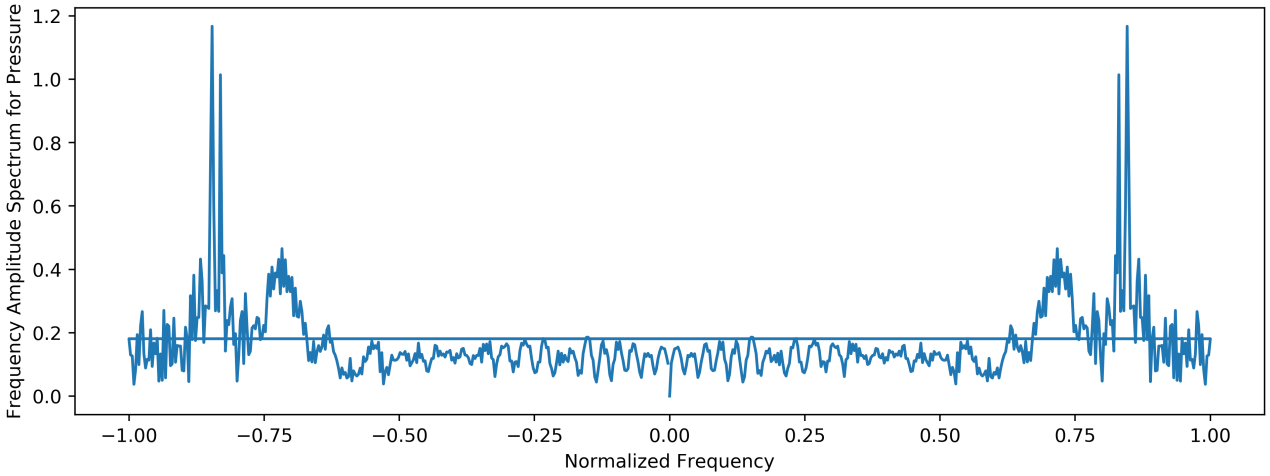

Figure (11) Figure 10 data in frequency normalized domain

4. CONCLUSIONS

The reactingFoam solver presented very promising preliminary results for the liquid rocket combustion chamber tested in this work. The pressure fluctuation obtained were expected and are in conformance with the extensive experimental data present in the works (Harrje (1972) and Young (1995)). The pressure oscillations are related with the acoustic waves of the gases in the liquid rocket engine, causing the instabilities and finally, the catastrophic failures. Using the predictor of acoustic waves, one can project a liquid rocket engine with a geometry in order to diminish these fluctuations or to eliminate them. The results obtained for the variations of the speed values show the perturbations in the fluid flow. As expected these fluctuations coupled with the pressure oscillations and consequently raise the instability in the rocket combustion chamber.

These fluctuations can be first visualized in the flow development, Figure 4 and 8. These results show a very good agreement with the literature a transient simulation of a combustion chamber. Also allow the visualization of the turbulence process, Figures 5 and 9, and most important the vorticities. Finally, it allows the authors to conclude the relevance of the solver uses for prevision of the reactive flow development.

The plots show that the oscillations patters for both velocity and pressure follow the chemical events, there is a well-posed peak in the two graphs and stable oscillation pattern. This stable oscillation pattern occurs because of the non-external excited combustion, that is proper of a combustion chamber in a static test. The transformation of the patterns in the frequency domain, Figures 11 and 7, allows a closer view of the similarity between pressure and speed. It is plausible as it is expected that the two process are coupled.

Further development is expected in future works to analyze the chemical reactions oscillation data, that has been obtained in the simulation. Other important features are the correlation between the pressure oscillations and the heat transfer oscillation.

5. REFERENCES

Chen, Y.S., Chou, T., Gu, B., Wu, J., Wu, B., Lian, Y. and Yang, L., 2011. "Multiphysics simulations of rocket engine combustion". *Computers & Fluids*, Vol. 45, No. 1, pp. 29–36.

Cheng, G.C. and Farmer, R., 2006. "Real fluid modeling of multiphase flows in liquid rocket engine combustors". *Journal of propulsion and power*, Vol. 22, No. 6, pp. 1373–1381.

Conaire, M., Curran, H.J., Simmie, J.M., Pitz, W.J. and Westbrook, C.K., 2004. "A comprehensive modeling study of hydrogen oxidation". *International journal of chemical kinetics*, pp. 603–622.

Crocco, L., 1953. "High-frequency combustion instability in rocket motor with concentrated combustion". *Journal of the American Rocket Society*, Vol. 23, No. 5, pp. 301–313.

Gonzalez, E., 2017. "Numerical simulations of thermoacoustic combustion instabilities in the volvo combustor". In *53rd AIAA/SAE/ASEE Joint Propulsion Conference*. p. 4686.

Harrje, D.T., 1972. "Liquid propellant rocket combustion instability".

Invigorito, M., Cardillo, D. and Ranuzzi, G., 2014. "Application of openfoam for rocket design". In *9th OpenFOAM Workshop, Zagreb, Croatia*.

Moukalled, F., Mangani, L. and Darwish, M., 2015. *The Finite Volume Method in Computational Fluid Dynamics: An Advanced Introduction with OpenFOAM® and Matlab*. Fluid Mechanics and Its Applications. Springer International

Publishing. ISBN 9783319168746. URL https://books.google.com.br/books?id=GYRgCgAAQBAJ.

Noiray, N., Durox, D., Schuller, T. and Candel, S., 2008. "A unified framework for nonlinear combustion instability analysis based on the flame describing function". *Journal of Fluid Mechanics*, Vol. 615, pp. 139–167.

Smirnov, N., Betelin, V., Shagaliev, R., Nikitin, V., Belyakov, I., Deryuguin, Y.N., Aksenov, S. and Korchazhkin, D., 2014. "Hydrogen fuel rocket engines simulation using logos code". *International journal of hydrogen energy*, Vol. 39, No. 20, pp. 10748–10756.

Summerfield, M., 1951. "A theory of unstable combustion in liquid propellant rocket systems". *Journal of the American Rocket Society*, Vol. 21, No. 5, pp. 108–114.

Tao, L. and Dongmei, Z., 2012. "Numeric simulation and analysis of h 2-o 2 premixed combustion based on openfoam". In *Robotics and Applications (ISRA), 2012 IEEE Symposium on*. IEEE, pp. 27–30.

Wang, Z., 2016. *Internal Combustion Processes of Liquid Rocket Engines: Modeling and Numerical Simulations*. Wiley. ISBN 9781118890042. URL https://books.google.com.br/books?id=lM0vDAAAQBAJ.

Young, V., 1995. *Liquid Rocket Engine Combustion Instability*. Ingenieria de transportes y aeronautica. American Institute of Aeronautics & Astronautics. ISBN 9781600864186. URL https://books.google.com.br/books?id=sobvSF82RVAC.

6. RESPONSIBILITY NOTICE

The authors are the only responsible for the printed material included in this paper.